

IV. NOTES: TRICKS OF THE TRADE – EFFICIENT CALCULATIONS

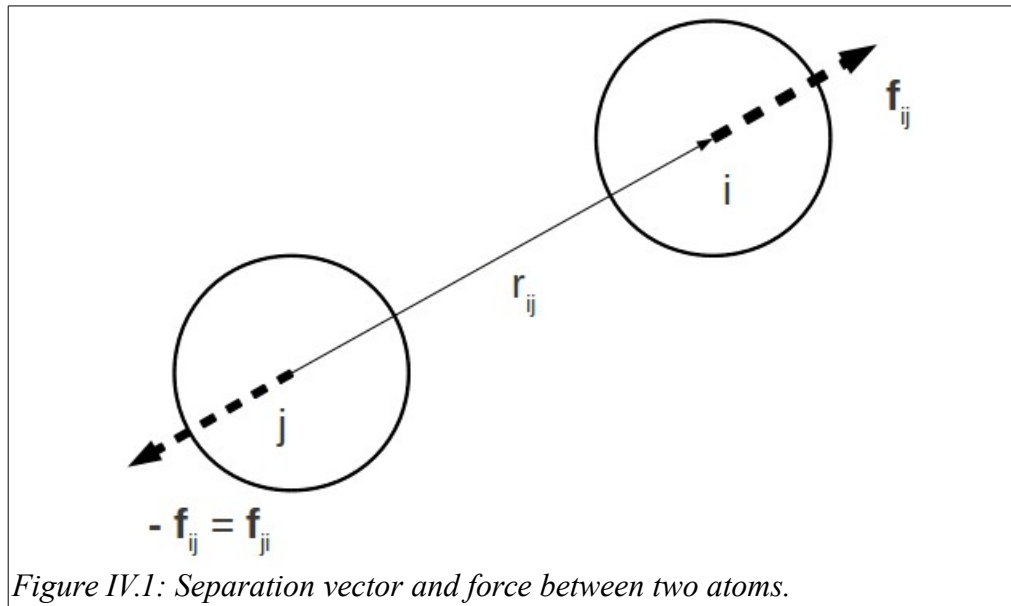
1. Forces

Different computational equipment have different relative efficiency of mathematical operations. However, the consideration of these efficiencies is very important in deciding the algorithms to be used. In general, square roots, logarithms, and trigonometric functions are an order of magnitude more computationally expensive than addition and multiplication. Thus, when calculating forces and potential energies of configurations (the heart of molecular dynamics simulation programs) we should avoid the more expensive operations in favor of efficiency. Great care must be taken to make this particular section of code as efficient as possible.

Consider an atomic system with pairwise potentials. For particles i and j the force on atom i due to atom j is:

$$\mathbf{f}_{ij} = -\nabla_{\mathbf{r}_i} V(r_{ij}) = -\nabla_{\mathbf{r}_{ij}} V(r_{ij}). \quad (1)$$

This force is directed along the interatomic vector $\mathbf{r}_{ij} = \mathbf{r}_i - \mathbf{r}_j$ as shown in Figure IV.1 and it can be



shown that

$$\mathbf{f}_{ij} = -\frac{1}{r_{ij}} \left(\frac{dV(r_{ij})}{dr_{ij}} \right) \mathbf{r}_{ij} = -\frac{w(r_{ij})}{r_{ij}^2} \mathbf{r}_{ij}. \quad (2)$$

This equation makes it clear that if $V(r_{ij})$ is an even function of r_{ij} , then the force vector can be calculated without ever working out the absolute magnitude of \mathbf{r}_{ij} since r_{ij}^2 will do. The function $w(r_{ij})$

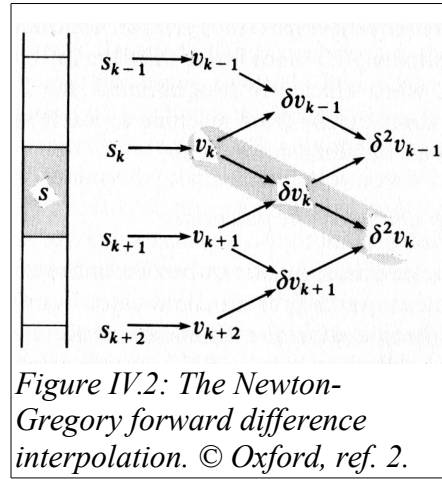
is the pair virial function

$$w(r_{ij}) = -\mathbf{r}_{ij} \cdot \mathbf{f}_{ij}. \quad (3)$$

If $V(r_{ij})$ is even in r_{ij} , then so is $w(r_{ij})$. Usually, V , w , and \mathbf{f} are calculated within a double loop over all pairs i and j . The force on particle j is calculated from the force in i by exploiting Newton's third law.

2. Potential Interpolation

As potentials used in simulations become more complicated, a direct evaluation of the potential and forces can be avoided by using a prepared table. The table is constructed once, at the beginning of the simulation program, and the potential and force are calculated as functions of $s=r_{ij}^2$. For a given table evaluated at certain values of s , a potential for an arbitrary particle separation r_{ij} is then found by interpolating known values of the potential. There are a variety of interpolation algorithms, but as an example let's use the Newton-Gregory forward difference method. Suppose we have tabulated a function $V(s)$, i.e. we have a set of values $V_1 = V(s_1)$, $V_2 = V(s_2)$, etc. at equal intervals δs . Define the first differences $\delta V_k = V_{k+1} - V_k$ and the second differences $\delta^2 V_k = \delta V_{k+1} - \delta V_k$. If we have a value s lying between the table values s_k and s_{k+1} , then $V(s)$ may be interpolated from the values V_k , δV_k , and $\delta^2 V_k$ (see Figure IV.2).



Setting $\xi = (s - s_k)/\delta s$ we have

$$V(s) \approx V_k + \xi \delta V_k + \frac{1}{2} \xi(\xi - 1) \delta^2 V_k. \quad (4)$$

In MD we also need the forces. We may compute these by constructing a separate table of values of the function $w(r_{ij})/r_{ij}^2$, which enters into the force calculation through equation 2. It is simpler, however, to note that this function is given by

$$\frac{w(r_{ij}^2)}{r_{ij}^2} = \frac{w(s)}{s} = 2 \frac{dV}{ds} \quad (5)$$

and obtain it by differentiation of equation 4. Great care must be put in choosing the table spacing as the success of this method relies on that choice. Typically, $\delta s = \delta r_{ij}^2 = 0.01 r_m^2$, where r_m is the position of the potential minimum, produces a sufficiently fine grid for use in MD simulations.

3. Potential Truncation

3.1. Minimum Image Convention

The heart of a MD program involves the calculation of the potential energy of a particular configuration. When using periodic boundary conditions we have to consider the interaction of the particles with their images. Consider how we would calculate the force on particle 1 (see Figure IV.3) assuming pairwise additivity.

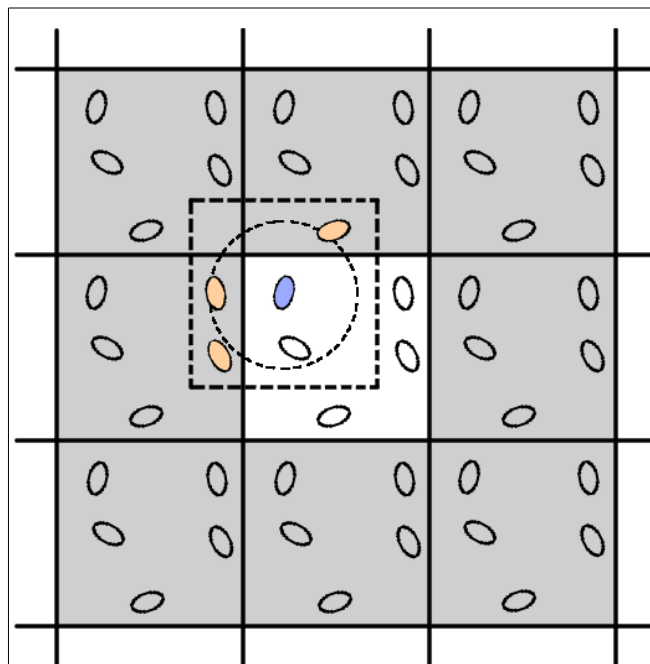


Figure IV.3: Minimum image convention in a two-dimensional system. The central box contains five particles. The “box” constructed with particle 1 (blue) at its center also contains five particles. The dashed circle represents a potential cutoff.

We must include interactions between particle 1 (blue) and every other particle j (white) in the simulation box. There are $N-1$ terms in this sum. However, in principle, we must also include all interactions between particle 1 and all images in neighboring cells that lie surrounding the central box. This is an infinite number of terms, and of course is impossible to calculate in practice. For a short-range potential energy function, we may restrict this summation by making an approximation. Consider particle 1 to rest at the center of a region which has the same size and shape as the basic simulation box. Particle 1 interacts with all the particles whose center lie within this region, that is with the closest periodic images of the other $N-1$ particles. This is called the *minimum image convention*. For example,

in Figure IV.3 particle 1 interacts with the white particle inside the dashed box as well as with the orange image particles.

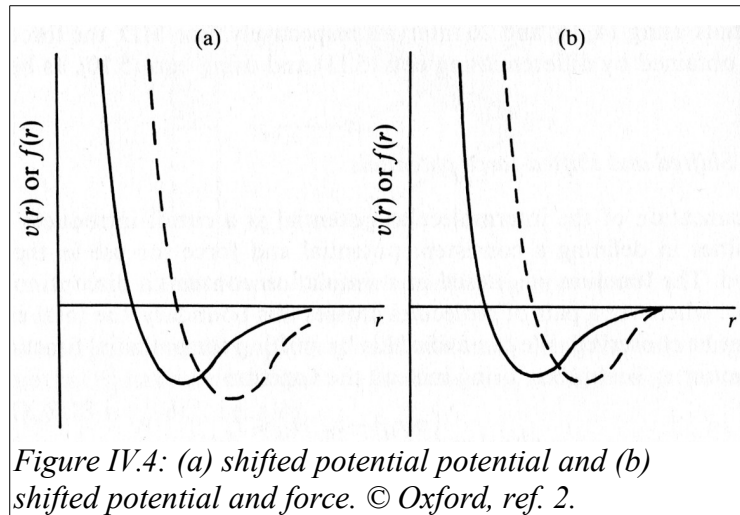
In the minimum image convention then the calculation of the potential energy due to pairwise-additive interactions involves $N(N-1)/2$ terms.

3.2. Shifted and Shifted-force Potentials

One easy way to avoid the $O(N^2)$ calculation of interactions over all pairs mentioned in the previous section is to introduce a distance cutoff, r_c , beyond which two particles will be considered too far to “feel” each other (dashed line in Figure IV.3). This truncation, however, introduces some difficulties in defining a consistent potential and force for use in the MD method. The function $V(r_{ij})$ used in a simulation then would contain a discontinuity at the cutoff $r_{ij} = r_c$: whenever a pair of particles cross this boundary, the total energy will not be conserved. We can avoid this by shifting the potential function by an amount $V_c = V(r_c)$, i.e. using instead the function

$$V^s(r_{ij}) = \begin{cases} V(r_{ij}) - V_c & r_{ij} \leq r_c \\ 0 & r_{ij} > r_c \end{cases} \quad (6)$$

shown in Figure IV.4(a). The small additional term is constant for any pair interaction, and does not affect the forces, and hence the equations of motion of the system. However, its contribution to the total energy varies from time step to time step, since the total number of pairs within cutoff range varies. This term should certainly be included in the calculation of the total energy, thus creating a modified



total energy over which the conservation law should apply. However, there is a further problem. The force between a pair of particles is still discontinuous at $r_{ij} = r_c$. As such, a force would have a value equivalent to the derivative of the potential for $r_{ij} \leq r_c$ but be zero for $r_{ij} > r_c$. This will certainly cause instabilities in the numerical solution of the differential equations. To avoid this difficulty, we can use the “shifted-force potential” in which a small linear term is added to the potential, so that its derivative is zero at the cutoff distance, as shown in equation 7

$$V^{sf}(r_{ij}) = \begin{cases} V(r_{ij}) - V_c - \left(\frac{dV(r_{ij})}{dr_{ij}} \right)_{r_{ij}=r_c} (r_{ij} - r_c) & r_{ij} \leq r_c \\ 0 & r_{ij} > r_c \end{cases} \quad (7)$$

The discontinuity now appears in the gradient of the force, not in the force itself. The shifted-force potential for the LJ case is shown in Figure IV.4(b). The force goes smoothly to zero at the cutoff r_c , removing problems in energy conservation and any numerical instability in the equations of motion. Of course, the difference between the shifted-force potential and the original potential means that the simulation no longer corresponds to the desired model liquid. However, the thermodynamic properties of a fluid of particles interacting with the unshifted potential can be recovered from the shifted-force potential simulation results by using perturbation schemes (not covered in this course).

4. Neighbor Lists

In general, when we are checking distances between particles we loop over all pairs. This is a process that again scales as N^2 operations since we have to consider all particle pairs. This is true even when using a cutoff distance for the interaction potential, since the cutoff only decides on whether there will be a calculated interaction but does not preclude the initial calculation of the distance between particles. To avoid the N^2 examination of pairs then we use a technique that keeps a list of the neighbors of a particular particle, which is updated at intervals. Between updates of the neighbor list, the program does not check through all the j particles, but just those appearing on the list. The number of pair separations explicitly considered is reduced. This saves time in looping through j , minimum imaging, calculating r_{ij}^2 , and checking against the cutoff, for all those particles not on the list.

4.1. Verlet Neighbor List

In the original Verlet method, the potential cutoff sphere, or radius r_c , around a particular particles is

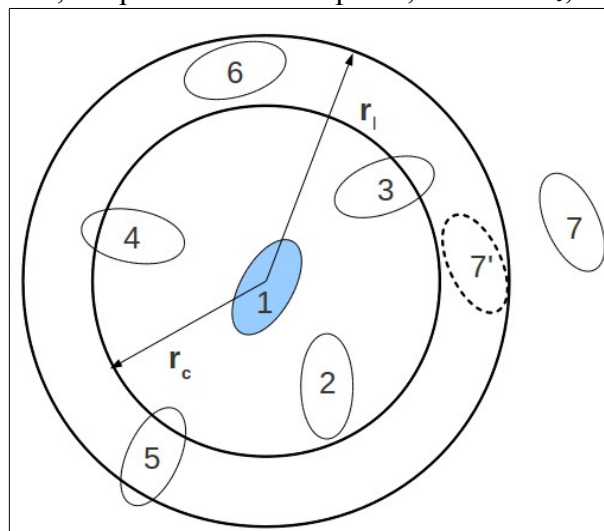


Figure IV.5: The cutoff sphere, and its skin, around a particle 1. Particles 2, 3, 4, 5, and 6 are on the list of particle 1 while particle 7 is not. Only molecules 2, 3, and 4 are within the range of the potential at the time the list is constructed.

surrounded by a “skin”, to give a large sphere of radius r_i , as shown in Figure IV.5. At the first step in a simulation, a list is constructed of all the neighbors of each particle, for which the pair separation is within r_i . These neighbors are stored in a large array of dimension roughly $4\pi r_i^3 \rho N/6$. Over the next few time steps, the array is used in the force/energy evaluation routine. From time to time, the neighbor list is reconstructed, and the cycle is repeated. For this algorithm to be successful the skin around r_c has to be chosen to be thick enough so that between reconstructions a particle, such as particle 7 in Figure IV.5, which is not on the list of particle 1, cannot penetrate through the skin into the important r_c sphere. Particles such as 3 and 4 can move in and out of this sphere, but since they are on the list of particle 1, they are always considered regardless, until the list is next updated.

The interval between updates of the table is often fixed at the beginning of the program, and intervals of 10 to 20 steps are quite common. Also, as the sphere radius r_i is increased, the frequency of updates of the neighbor list will decrease. However, with a large list, the efficiency of the non-update steps will decrease.

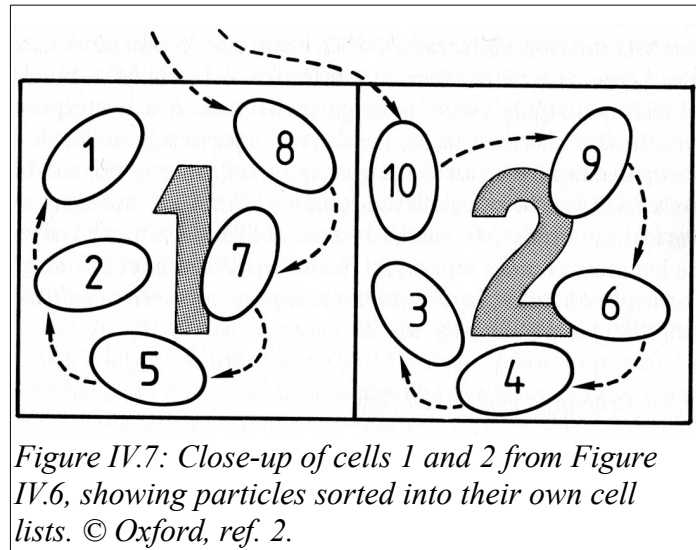
4.2. Cell Structures

1	2	3	4	5
6	7	8	9	10
11	12	13	14	15
16	17	18	19	20
21	22	23	24	25

Figure IV.6: two dimensional representation of the cell method. The central box is divided into $M \times M$ cells ($M=5$).

As the size of the system increases, the conventional neighbor list becomes too large to store easily, and the logical testing of every pair in the system is inefficient. An alternative method of keeping track of neighbors for large systems is the cell index method. The cubic simulation box is divided into a regular lattice of $M \times M \times M$ cells. A two-dimensional representation of this is shown in Figure IV.6.

These cells are chosen such that the side of the cell $l = L/M$ is greater than the cutoff distance for the forces, r_c . For the two-dimensional example in the figure, the neighbors of any molecule in cell 13 are to be found in the cells 7, 8, 9, 12, 13, 14, 17, 18, and 19. If there is a separate list of particles in each of those cells, then searching through the neighbors is a rapid process, as shown in Figure IV.7.

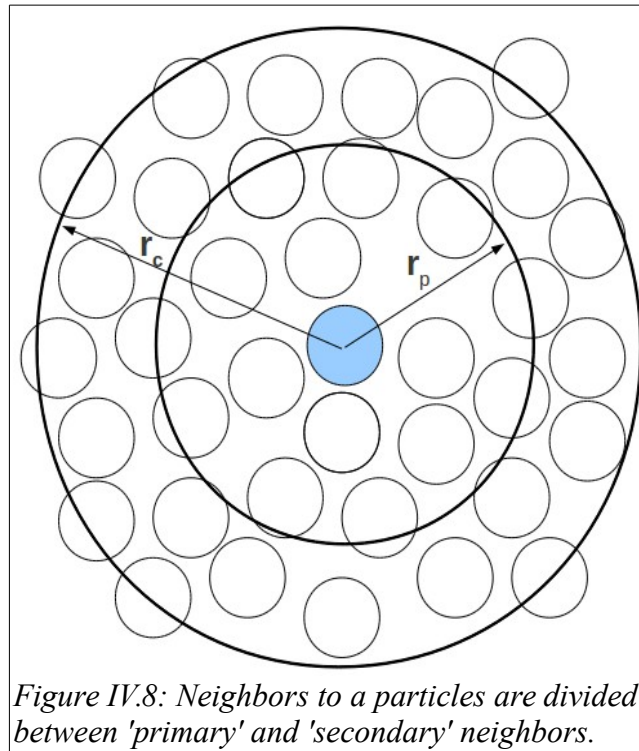


For the example shown in Figure IV.6, there are approximately $N_c = N/M^2$ particles in each cell that in three-dimensions is $N_c = N/M^3$.

Using the cell structure in two dimensions we need only examine $9NN_c$ pairs (or just $4.5NN_c$ if we take advantage of the 3rd law). This contrasts with N^2 (or $N(N-1)/2$) for the brute force approach. When the cell structure is used in three dimensions, then we compute $27NN_c$ interactions ($13.5NN_c$) as compared with N^2 (or $N(N-1)/2$).

5. Multiple Time Step Methods

After implementing the neighbor lists method, further speed-ups can be achieved by cutting down the time spent actually evaluating forces between pairs within the cutoff range specified in the neighbor lists. In the multiple time step methods we typically split the space within the cutoff into two groups. In Figure IV.8 we show the neighbors to a particular atom (at the center) which are split into two groups: *primary* neighbors, which lie within a distance r_p of the reference particle, and *secondary* neighbors, which are at a distance between r_p and r_c from the reference particle. In this way, the total force \mathbf{f}_i on particle i is separated into a primary component \mathbf{f}_i^p due to the close neighbors, and a secondary component \mathbf{f}_i^s from the more remote neighbors. Typically, for a LJ fluid, r_p would be chosen to lie between σ and 1.5σ . The motion of particle i is dominated by a rapidly changing primary force resulting from collisions with the nearest neighbor 'cage'. The secondary force is smaller, and changes more slowly with time. The multiple time step method takes advantage of this separation, and aims to calculate the secondary pair interactions less frequently than the more important primary ones.



6. Long-range forces

A long-range force is often defined as one in which the spatial interaction falls off no faster than r^{-d} where d is the dimensionality of the system. In this category are the charge-charge interaction between ions [$V_{zz}(r) \sim r^{-1}$] and the dipole-dipole interaction between molecules [$V_{\mu\mu}(r) \sim r^{-3}$]. These forces are a serious problem as their range is greater than half the box length for a typical simulation. The brute force approach is to increase the size of the central box L to hundreds of nanometers so that the screening by neighbors would diminish the effective range of the potentials. But this solution is still impractical due to hardware constraints since the time required to run such a simulation is approximately proportional to N^2 , i.e. L^6 .

Simple approaches to deal in particular with $V_{zz}(r)$ are usually flawed. Straightforward spherical truncation of this potential can be ruled out. The resulting sphere around a given ion could be charged, since the number of anions and cations need not balance at any instant. The tendency of ions to migrate back and forth across the spherical surface would create artificial effects at $r = r_c$. This can be countered by distributing a new charge over the surface of the sphere, equal in magnitude and opposite in sign to the net charge of the sphere, so as to guarantee local electric neutrality. This is rather like shifting the potential and it can be shown that the results approximate those obtained with the Ewald sum for rather large systems, but some undesirable structural effects are inevitable.

Applying a basic minimum image method corresponds to cutting off the potential at the surface of a cube surrounding the ion in question (see Section IV.3.1 and Figure IV.3). This cube will be electrically

neutral. However, the drawback is that similarly charged ions will tend to occupy positions in opposite corners of the cube: the periodic image structure will be imposed directly on what should be an isotropic liquid, and this results in a distortion of the liquid structure.

There are two typical methods to tackle these problems: a lattice method dictated by the *Ewald sum* that include the interaction of an ion or molecule with all its periodic images, and the *Reaction Field method* that assumes that the interaction from particles beyond a cutoff distance can be handled in an average way using macroscopic electrostatics. The Ewald sum will tend to overemphasize the periodic nature of the model fluid while the reaction field method will tend to overemphasize the continuum nature of a polar fluid and require an *a priori* estimate of the relative permittivity. Both methods use well-known ideas from the theory of electrostatics. In particular, a charge distribution within a spherical cavity polarizes the surrounding medium. This polarization, which depends upon the relative permittivity of the medium, has an effect on the charge distribution in the cavity.

6.1. The Ewald Sum

The Ewald sum is a technique for efficiently summing the interaction between an ion and all its periodic images. For an ion centered in a box with images surrounding it, the total potential energy can be written as

$$V_{zz} = \frac{1}{2} \sum_{\mathbf{n}}' \left(\sum_{i=1}^N \sum_{j=1}^N z_i z_j |\mathbf{r}_{ij} + \mathbf{n}|^{-1} \right) \quad (8)$$

where z_i, z_j are the charges and the $4\pi\epsilon_0$ factors have been omitted. The sum over \mathbf{n} is the sum over all simple cubic lattice points, $\mathbf{n} = (n_x L, n_y L, n_z L)$ with n_x, n_y, n_z integers. This vector reflects the shape of the basic box. The prime indicates that we omit $i=j$ for $\mathbf{n}=0$. For long-range potentials, this sum is conditionally convergent, i.e. the result depends on the order in which we add up the terms. A natural choice is to take boxes in order of their proximity to the central box. The unit cells are added in sequence: the first term has $|\mathbf{n}|=0$, i.e. $\mathbf{n}=(0,0,0)$; the second term, $|\mathbf{n}|=L$, comprises the six boxes centered at $\mathbf{n}=(\pm L, 0, 0), (0, \pm L, 0), (0, 0, \pm L)$, etc. As we add further terms to the sum, we are building up our infinite system in roughly spherical layers (see Figure IV.9). With this approach we must specify the nature of the medium surrounding the sphere, in particular its relative permittivity (dielectric constant) ϵ_s . The results for a sphere surrounded by a good conductor such as a metal ($\epsilon_s = \infty$) and for a sphere surrounded by vacuum ($\epsilon_s = 1$) are different, as shown in equation 9

$$V_{zz}(\epsilon_s = \infty) = V_{zz}(\epsilon_s = 1) - \frac{2\pi}{3L^3} \left| \sum_i z_i \mathbf{r}_i \right|^2. \quad (9)$$

Equation 9 applies in the limit of a very large sphere of boxes. In the vacuum, the sphere has a dipolar layer on its surface: the last term of equation 9 cancels this. For the sphere in a conductor there is no such layer. The Ewald method is a way of efficiently calculating $V_{zz}(\epsilon_s = \infty)$. Equation 9 enables us to use the Ewald sum in a simulation where the large sphere is in a vacuum, if this is more convenient.

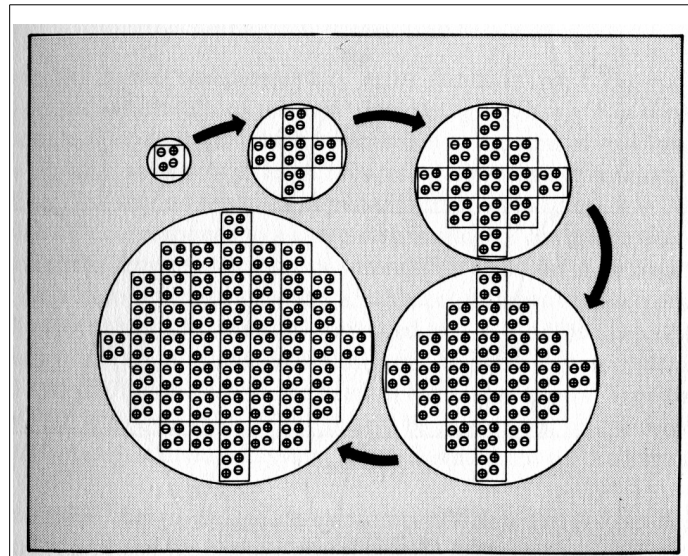


Figure IV.9: Building up a sphere of simulation boxes for two pairs of ions. The shaded external region represents the external dielectric continuum of relative permittivity ϵ_s . © Oxford, ref. 2.

In practice, at any point during the simulation, the distribution of charges in the central cell constitutes the unit cell for a neutral lattice which extends throughout space. In the Ewald method, each point charge is surrounded by a charge distribution of equal magnitude and opposite sign, which spreads out radially from the charge. This distribution is conveniently taken to be Gaussian

$$\rho_i^z(\mathbf{r}) = z_i \kappa^3 \exp(-\kappa^2 r^2) / \pi^{3/2} \quad (10)$$

where the arbitrary parameter κ determines the width of the distribution, and \mathbf{r} is the position relative to the center of the distribution. This extra distribution acts like an ionic atmosphere, to screen the interaction between neighboring charges. The screened interactions are now short-ranged, and the total screened potential is calculated by summing over all the particles in the central cube and all their images in the real space lattice of image boxes. This is illustrated in Figure IV.10(a).

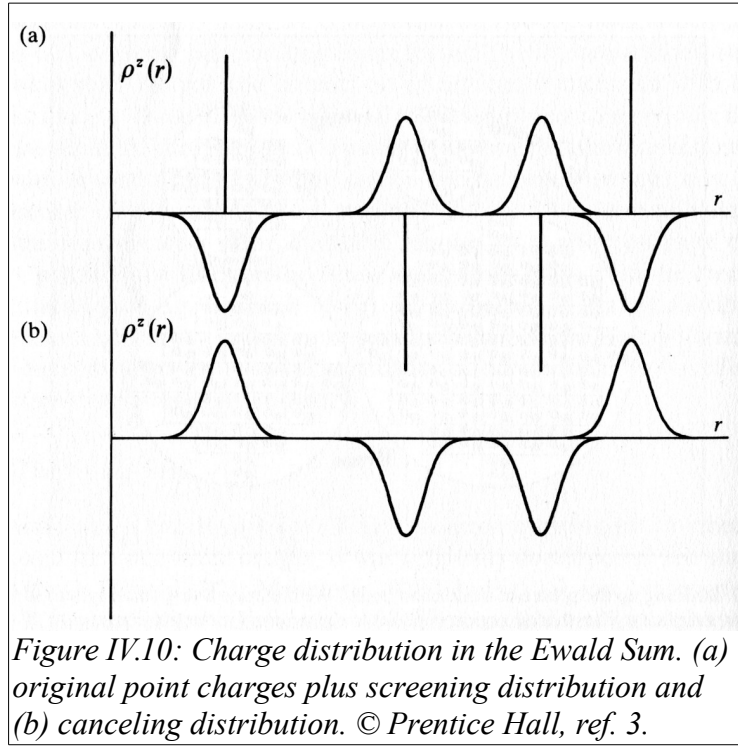


Figure IV.10: Charge distribution in the Ewald Sum. (a) original point charges plus screening distribution and (b) canceling distribution. © Prentice Hall, ref. 3.

A charge distribution of the same sign as the original charge, and the same shape as the distribution $\rho_i^z(\mathbf{r})$ is also added (Figure IV.10(b)). This canceling distribution reduces the overall potential to that due to the original set of charges. The canceling distribution is summed in reciprocal space. In other words, the Fourier transforms of the canceling distributions (one for each original charge) are added, and the total transformed back into real space. There is an important correction: the recipe includes the interaction of the canceling distribution centered at \mathbf{r}_i with itself, and this self term must be subtracted from the total. Thus, the final potential energy will contain a real space sum plus a reciprocal space sum minus a self-term plus the surface term already discussed for the larger sphere enclosing the periodic boxes. The final result is

$$\begin{aligned}
 V_{zz}(\epsilon_s = 1) = & \frac{1}{2} \sum_{i=1}^N \sum_{j=1}^N \left(\sum_{|\mathbf{n}|=0}^{\infty'} z_i z_j \frac{\text{erfc}(\kappa |\mathbf{r}_{ij} + \mathbf{n}|)}{|\mathbf{r}_{ij} + \mathbf{n}|} \right. \\
 & \left. + (1/\pi L^3) \sum_{\mathbf{k} \neq 0} z_i z_j (4\pi^2/k^2) \exp(-k^2/4\kappa^2) \cos(\mathbf{k} \cdot \mathbf{r}_{ij}) \right) \\
 & - (\kappa/\pi^{1/2}) \sum_{i=1}^N z_i^2 + (2\pi/3L^3) \left| \sum_{i=1}^N z_i \mathbf{r}_i \right|^2
 \end{aligned} \tag{11}$$

Here $\text{erfc}(x)$ is the complementary error function ($\text{erfc}(x) = (2/\pi^{1/2}) \times \int_x^\infty \exp(-t^2) dt$) which falls

to zero with increasing x . Thus, if κ is chosen to be large enough, the only term which contributes to the sum in real space is that with $n=0$, and so the first term reduces to the normal minimum image convention. The second term is a sum over reciprocal vectors $\mathbf{k} = 2\pi\mathbf{n}/L^2$. A large value of κ corresponds to a sharp distribution of charge, so that we need to include many terms in the k-space summation to model it. In a simulation, the aim is to choose a value of κ and a sufficient number of k-vectors, so that equation 11 give the same energy for typical liquid configurations.

In practice, κ is typically set to $5/L$, though the results turn out to be relatively insensitive to the choice, provided there are sufficient terms in $\sum_{\mathbf{n}}$. A spherical cutoff is imposed on this sum, so that $n \equiv |\mathbf{n}| \leq n_c$; typically n_c is about 5.

Imposing a cutoff on the real-space sum at r_c leads to an error of order $\exp(-\kappa^2 r_c^2)$; truncating the Fourier space sum at n_c produces an error of order $\exp(-\pi^2 n_c^2 / \kappa^2 L^2)$. Therefore, to obtain similarly sized errors in both the real and Fourier contributions to the energy, simply set

$$n_c = \kappa^2 r_c L / \pi . \quad (12)$$

For the case $r_c = L/2$, if $\kappa = 5/L$ we obtain a rather small $n_c = 25/2\pi \approx 4$. The actual number of terms in the sum is roughly $4\pi n_c^3/3$.

6.2. The Reaction Field Method

In the reaction field method, the field on a dipole in the simulation consists of two parts: the first is a short-range contribution from particles situated within a cutoff sphere or “cavity” \mathfrak{R} , and the second arises from particles outside \mathfrak{R} which are considered to form a dielectric continuum (ϵ_s) producing a reaction field within the cavity (see Figure IV.11).

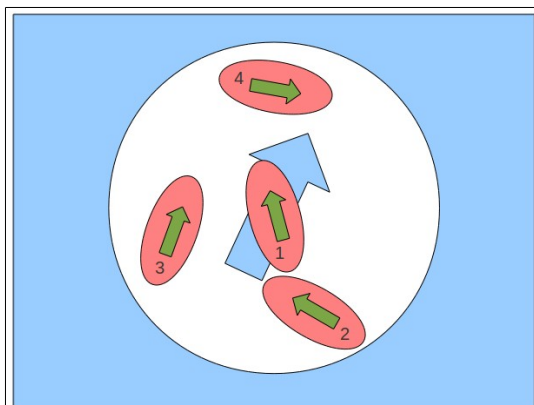


Figure IV.11: A cavity and reaction field. Particles 2, 3, and 4 interact directly with particle 1. The continuum polarized by the particles in the cavity produces a reaction field at 1 (shaded).

The size of the reaction field, the electrostatic field due to the surrounding dielectric, acting on particle

i is proportional to the moment of the cavity surrounding i ,

$$E_i = \frac{2(\varepsilon_s - 1)}{2\varepsilon_s + 1} \frac{1}{r_c^3} \sum_{j \in E} \mu_j \quad (13)$$

where μ_i are the dipoles of the neighboring particles, the summation extends over the particles in the cavity, including i , and r_c is the radius of the cavity. The contribution to the energy from the reaction field is $-\frac{1}{2}\mu_i \cdot E_i$. The torque on particle i from the reaction field is $\mu_i \times E_i$.

Whenever a particle enters or leaves the cavity surrounding another, a discontinuous jump occurs in the energy due to direct interactions within the cavity and in the reaction field contribution. These changes do not exactly cancel, and the result is poor energy conservation in MD. These problems may be avoided by tapering the interactions at the cavity surface: the explicit interactions between molecules i and j are weighted by a factor $f(r_{ij})$, which approaches zero continuously at $r_{ij} = r_c$. For example, linear tapering may be used;

$$f(r_{ij}) = \begin{cases} 1.0 & r_{ij} < r_t \\ (r_c - r_{ij})/(r_c - r_t) & r_t \leq r_{ij} \leq r_c \\ 0.0 & r_c < r_{ij} \end{cases} \quad (14)$$

where an appropriate value of r_t is $r_t = 0.95 r_c$. The contribution of the particle dipoles to the cavity dipole, and hence the reaction field, are correspondingly weighted.

The static reaction field is straightforward to calculate in a conventional MD simulation, and it involves only a modest increase in execution time. A potential difficulty with the reaction field method is the need for an *a priori* knowledge of the external dielectric constant (ε_s).

7. Dimensionless Units

It is often convenient to introduce a set of dimensionless, or reduced, MD units in terms of which all physical quantities will be expressed. There are several reasons for doing this, not the least being the ability to work with numerical values that are not too distant from unity, instead of the extremely small values normally associated with the atomic scale. Another benefit of dimensionless units is that the equations of motion are simplified because some, if not all, of the parameters defining the model are absorbed into the units. The most familiar reason for using such units is related to the general notion of scaling, namely, that a single model can describe a whole class of problems, and once the properties have been measured in dimensionless units they can easily be scaled to the appropriate physical units for each problem of interest. From a strictly practical point of view, the switch to such units removes any risk of encountering values lying outside the range that is representable by the computer hardware.

For MD studies using potentials based on the LJ form, the most suitable dimensionless units are defined by choosing σ , m , and ε to be the units of length, mass, and energy, respectively, and making the replacements:

- length: $r \rightarrow r\sigma$
- energy: $e \rightarrow e\epsilon$
- time: $t \rightarrow t\sqrt{m\sigma^2/\epsilon}$

The resulting form of the equation of motion, now in MD units, is

$$\ddot{\mathbf{r}}_i = 48 \sum_{j \neq i} \left(r_{ij}^{-14} - \frac{1}{2} r_{ij}^{-8} \right) \mathbf{r}_{ij} \quad (15)$$

The dimensionless kinetic and potential energies, per atom, are

$$E_k = \frac{1}{2N_m} \sum_{i=1}^{N_m} \mathbf{v}_i^2 \quad (16)$$

And

$$E_p = \frac{4}{N_m} \sum_{1 \leq i < j \leq N_m} (r_{ij}^{-12} - r_{ij}^{-6}) \quad (17)$$

where \mathbf{v}_i is the velocity.

The unit of temperature is ϵ/k_B , and since each translational degree of freedom contributes $k_B T/2$ to the kinetic energy, the temperature of a d-dimensional (d=2 or 3) system is

$$T = \frac{1}{dN_m} \sum_i \mathbf{v}_i^2 \quad (18)$$

We have set $k_B = 1$, so that the MD unit of temperature is now also defined. Strictly speaking, of the total dN_m degrees of freedom, d are eliminated because of momentum conservation, but if N_m is not too small this detail can be safely ignored.

If the model is intended to represent liquid argon, the relations between the dimensionless MD units and real physical units are as follows.

- Lengths are expressed in terms of $\sigma = 3.4 \text{ \AA}$.
- The energy units are specified by $\epsilon/k_B = 120K$, implying that $\epsilon = 120 \times 1.3806 \times 10^{-16} \text{ erg/atom}$.
- Given the mass of an argon atom $m = 39.95 \times 1.6747 \times 10^{-24} \text{ g}$, the MD time unit corresponds to $2.161 \times 10^{-12} \text{ s}$; thus a typical timestep size of $\Delta t = 0.005$ corresponds to approximately 10^{-14} s .
- Finally, if N_m atoms occupy a cubic region of edge length L , then a typical liquid density of 0.942 g/cm^3 implies that $L = 4.142 N_m^{1/3} \text{ \AA}$, which in reduced units amount to $L = 1.218 N_m^{1/3}$.